

This article was downloaded by:

On: 18 January 2011

Access details: *Access Details: Free Access*

Publisher *Taylor & Francis*

Informa Ltd Registered in England and Wales Registered Number: 1072954 Registered office: Mortimer House, 37-41 Mortimer Street, London W1T 3JH, UK



## International Journal of Polymeric Materials

Publication details, including instructions for authors and subscription information:

<http://www.informaworld.com/smpp/title~content=t713647664>

### Frequency and Temperature Dependence of Dielectric Properties of Au/Polyvinyl Alcohol (Co, Ni-Doped)/n-Si Schottky Diodes

Tuncay Tunç<sup>a</sup>; İbrahim Uslu<sup>b</sup>; İlbilge Dökme<sup>c</sup>; Şemsettin Altındal<sup>d</sup>; Habibe Uslu<sup>b</sup>

<sup>a</sup> Faculty of Education, Department of Science Education, Aksaray University, Aksaray, Turkey <sup>b</sup>

Faculty of Education, Department of Chemistry Education, Selçuk University, Konya, Turkey <sup>c</sup> Faculty

of Gazi Education, Department of Science Education, Gazi University, Ankara, Turkey <sup>d</sup> Faculty of Arts and Sciences, Department of Physics, Gazi University, Ankara, Turkey

Online publication date: 09 August 2010

**To cite this Article** Tunç, Tuncay , Uslu, İbrahim , Dökme, İlbilge , Altındal, Şemsettin and Uslu, Habibe(2010) 'Frequency and Temperature Dependence of Dielectric Properties of Au/Polyvinyl Alcohol (Co, Ni-Doped)/n-Si Schottky Diodes', *International Journal of Polymeric Materials*, 59: 10, 739 – 756

**To link to this Article:** DOI: 10.1080/00914037.2010.483215

**URL:** <http://dx.doi.org/10.1080/00914037.2010.483215>

PLEASE SCROLL DOWN FOR ARTICLE

Full terms and conditions of use: <http://www.informaworld.com/terms-and-conditions-of-access.pdf>

This article may be used for research, teaching and private study purposes. Any substantial or systematic reproduction, re-distribution, re-selling, loan or sub-licensing, systematic supply or distribution in any form to anyone is expressly forbidden.

The publisher does not give any warranty express or implied or make any representation that the contents will be complete or accurate or up to date. The accuracy of any instructions, formulae and drug doses should be independently verified with primary sources. The publisher shall not be liable for any loss, actions, claims, proceedings, demand or costs or damages whatsoever or howsoever caused arising directly or indirectly in connection with or arising out of the use of this material.

# Frequency and Temperature Dependence of Dielectric Properties of Au/Polyvinyl Alcohol (Co, Ni-Doped)/n-Si Schottky Diodes

Tuncay Tunç,<sup>1</sup> İbrahim Uslu,<sup>2</sup> İlbilge Dökme,<sup>3</sup>  
Şemsettin Altındal,<sup>4</sup> and Habibe Uslu<sup>2</sup>

<sup>1</sup>Faculty of Education, Department of Science Education, Aksaray University, Aksaray, Turkey

<sup>2</sup>Faculty of Education, Department of Chemistry Education, Selçuk University, Konya, Turkey

<sup>3</sup>Faculty of Gazi Education, Department of Science Education, Gazi University, Ankara, Turkey

<sup>4</sup>Faculty of Arts and Sciences, Department of Physics, Gazi University, Ankara, Turkey

The dielectric properties and AC conductivity of Au/polyvinyl alcohol (Co, Ni-doped)/n-Si Schottky diodes (SDs) were investigated in the frequency range 1 kHz–1 MHz and in the temperature range 80–400 K. The frequency and temperature dependence of dielectric constant ( $\epsilon'$ ), dielectric loss ( $\epsilon''$ ), loss tangent ( $\tan \delta$ ), AC electrical conductivity ( $\sigma_{ac}$ ) and the real and imaginary parts of the electric modulus ( $M'$  and  $M''$ ) were found to be a strong function of frequency and temperature. The values of  $\epsilon'$ ,  $\epsilon''$  and  $\tan \delta$  decrease with increasing frequency, while they increase with increasing temperature, especially above 275 K. The values of  $\sigma_{ac}$  increase with both increasing frequency and temperature. Such temperature-related behavior of  $\sigma_{ac}$  can be attributed to the high mobility of free charges at high temperature. Electric modulus formalism was also analyzed to obtain experimental dielectric data. The values of  $M'$  and  $M''$  increase with

Received 13 January 2010; accepted 12 March 2010.

Address correspondence to Tuncay Tunç, Faculty of Education, Department of Science Education, Aksaray University, Aksaray, Turkey. E-mail: tctunc@gmail.com

increasing frequency, while they decrease with increasing temperature. The interfacial polarization, which more easily occurs at low frequencies and high temperatures, consequently contributes to the improvement of the dielectric properties of SDs.

**Keywords** Au/PVA (Co, Ni-Doped)/n-Si, dielectric properties, electrospinning technique, polyvinyl alcohol, Schottky diode

## INTRODUCTION

Polymeric materials have been the subject of intense scientific and technological research because of their potential applications. In particular, conducting polymers have been extensively investigated in the area of electronics and optoelectronics due to their attractive properties [1,2]. Recently, the use of polymers as dielectrics has attracted attention in science and technology. Polymeric dielectric materials have been preferred by reason of their dielectric and physical properties over a wide range of temperatures and frequencies. Recently, there has been much interest in polymer blends and polymers doped with metal ions. The electrical properties of polymers doped with metal ions have been widely investigated by many researchers [3,4]. Among various polymers, poly(vinyl alcohol) (PVA), as one of the most important polymers, has recently received considerable interest, owing to its numerous potential applications in electronic components, such as Schottky diodes. Figure 1 shows the structure of PVA. PVA is an interesting synthetic polymer, because of its unique chemical and physical properties. PVA is a polyhydroxy polymer obtained via the hydrolysis of polyvinyl acetate, whose acetate groups are replaced by hydroxyls [5]. PVA polymer is soluble in water and other solvents, and is widely used in synthetic fiber, paper, contact lens, textile, coating, and binder industries, due to its excellent chemical and physical properties, nontoxicity, processability, good chemical resistance, wide range of crystallinity, good film formation capacity, complete biodegradability and high crystal modulus [6–9]. PVA is normally a poor electrical conductor; it

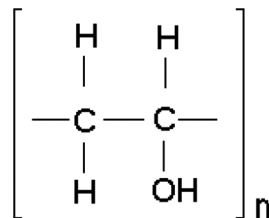


**Figure 1:** Chemical structure of PVA.

can become conductive upon blending and doping with some polymers and metal salt dopants [10,11]. The poor conducting properties of PVA are thought to be due to interactions between polymer chains via hydrogen bonding with hydroxyl groups. When a polymer is doped, the dopant can induce modifications in the molecular structure and hence the microstructural property of the polymer. In particular the transition metal salts and nanoparticle-doped polymers are considered to be a new class of organic materials, due to their considerable modification of physical properties, including microstructural, optical, electrical and thermal properties [11]. The electrical properties of polyvinyl alcohol with different dopant metal ions receive particular attention in potential device applications. Dielectric measurements such as dielectric constant  $\epsilon'$  and power factor  $\tan \delta$  are significantly affected by the presence of another polymer or a dopant in the polymer [12–14]. Nonetheless, there is considerable interest in the electric and dielectric properties of nanofiber polymer composite films, and the measurement of their properties has become increasingly important and necessary. One of the applications of the polymer composite films is SDs. SDs on metal-semiconductor substrates are used as parametric amplifiers, frequency multipliers, mixer diodes and generators. Polymer composite nanofiber films can be prepared by many methods; the present study used an electrospinning technique, which utilizes electrical force to produce polymer fibers. Nanofiber metal oxides have been the subject of intense research, because of their potential applications in many fields, including electronics, photonics and sensing [15–18]. In this study, polyvinyl alcohol (Co, Ni-doped) film was used as an interfacial layer between metal and semiconductor. PVA doped with different ratios of nickel and zinc was produced and PVA/(Co, Ni) nanofiber film on a silicon semiconductor was fabricated by the use of an electrospinning technique. In the previous study, we fabricated Au/polyvinyl alcohol (Ni, Zn-doped)/n-Si Schottky diodes, and temperature-dependent electrical and dielectric properties of the diode were calculated from the capacitance–voltage (C–V) and conductance–voltage (G/w–V) measurements in the temperature range of 80–400 K [19]. The dielectric constant ( $\epsilon'$ ), dielectric loss ( $\epsilon''$ ), dielectric loss tangent ( $\tan \delta$ ) and the AC electrical conductivity ( $\sigma_{ac}$ ) obtained from the measured capacitance and conductance were studied for Au/PVA (Ni, Zn-doped)/n-Si SDs. Experimental results showed that the values of  $\epsilon'$ ,  $\epsilon''$  and  $\tan \delta$  were a strong function of the temperature. This paper presents a detailed study of the electrical and dielectric properties Au/polyvinyl alcohol (Co, Ni-doped)/n-Si SDs in the frequency range 1 kHz–1 MHz at temperatures between 80–400 K. The admittance technique was used to determine the dielectric constant ( $\epsilon'$ ), dielectric loss ( $\epsilon''$ ), loss tangent ( $\tan \delta$ ), AC electrical conductivity ( $\sigma_{ac}$ ), and the electric modulus of the structure [20,21].

## EXPERIMENTAL

### Preparation of PVA/Co, Ni Acetate Composite

The experiments were carried out with PVA (Merck) with an average molecular weight of 72000, nickel acetate,  $\text{Ni}(\text{CH}_3\text{COO})_2 \cdot 4\text{H}_2\text{O}$  (Merck, 99% purity), zinc acetate (Sigma-Aldrich, 99.5% purity), and deionized ultra-pure water. PVA is sparingly soluble in water. Therefore, the aqueous 10% PVA solution was prepared by constant mixing at  $80^\circ\text{C}$  for 3 h. 0.5 g of cobalt acetate and 0.25 g of nickel acetate were dissolved in an appropriate amount of deionized water. These solutions were mixed with 10 g of PVA. After vigorous stirring for 2 h at  $50^\circ\text{C}$ , a viscous solution of PVA/(Co-Ni) acetates was obtained.

### Fabricating Schottky Diodes and Temperature and Frequency Dependence Capacitance and Conductance Measurements

The Au/PVA (Co, Ni-doped)n-Si SDs were fabricated using n-type (phosphor-doped) single crystal silicon wafer with (111) surface orientation, having thickness of  $350\ \mu\text{m}$ , 2 inch (5.08 cm) diameter and  $\cong 0.7\ \Omega\text{cm}$  resistivity. Before making contact, the Si wafer was first cleaned in a mix of a peroxide-ammoniac solution and then in  $\text{H}_2\text{O} + \text{HCl}$  solution for 10 min. It was then rinsed thoroughly for 15 min in an ultrasonic bath using deionized water with resistivity of  $18\ \text{M}\Omega\text{cm}$ . After surface cleaning, high purity 999.999 Au with a thickness of approximately  $2000\ \text{Å}$  was thermally evaporated onto the entire back side of the Si wafer in a high vacuum system at a pressure of approximately  $10^{-6}$  Torr. The ohmic contacts were formed by annealing them for 5 min at  $450^\circ\text{C}$  in a  $\text{N}_2$  atmosphere. The nanofibers were prepared by the use of an electrospinning technique. The electrospinning system is composed of (i) a high-voltage power generator, (ii) a syringe, (iii) a collector made of a metallic material, and (iv) a dosage pump (New Era Pump Systems, Inc.). The composite solution for spinning was loaded into a 10 mL hypodermic stainless steel syringe with a needle (0.8 mm in diameter and 38 mm length) connected to a digitally controlled pump (New Era) which provides a constant flow rate of 0.02 ml/h. The metal tip of the syringe is connected to the power supply (SP-30P, Gamma High Voltage Research) and the other end is connected to the collector wrapped with Al foil. A Si wafer was placed on the aluminum foil. The distance between the metal tip and the collected was kept at 15 cm. Upon applying a high voltage of 20 kV to the needle, a fluid jet was ejected from the tip. A simple illustration of the electrospinning system is given in Figure 2. After the PVA (Co, Ni-doped) film was deposited onto the Si wafer as a nonwoven mat by spinning, the Schottky/rectifier contacts were coated by evaporation with Au dots with a diameter

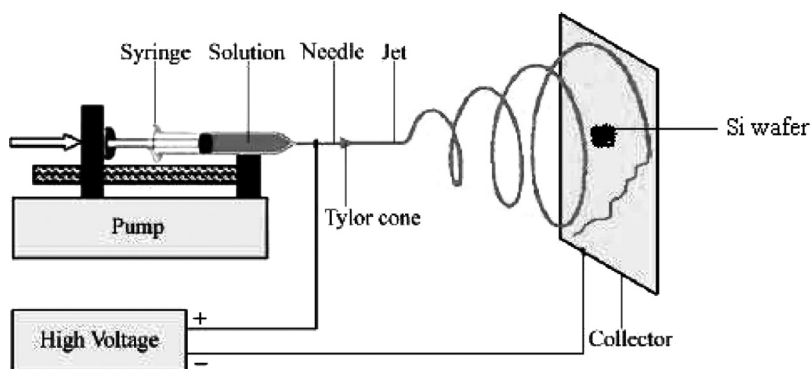


**Figure 2:** Schematic representation of the electrospinning process.

of approximately 1.0 mm (diode area =  $7,85 \times 10^{-3} \text{ cm}^2$ ). Figure 3 shows the typical device structure used in this work.

The  $C-V$  and  $G/\omega-V$  measurements were measured in the frequency range of 1 kHz–1 MHz and temperature range of 80–400 K (at 1 MHz), using a HP 4192A LF impedance analyzer (5 Hz–13 MHz). A small sinusoidal test signal of 20 mV<sub>p-p</sub> from the external pulse generator was applied to the sample in order to meet the requirement. The sample temperature was continuously monitored using a temperature-controlled Janes vpf-475 cryostat, which enables measurements in the range of 77–450 K. All measurements were carried out with the help of a microcomputer through an IEEE-488 AC/DC converter card.

Fiber formation and morphology of the electrospun Co-Ni/PVA fibers were determined using a scanning electron microscope (SEM) Quanto 400 FEI MK-2. The diameter of nonwoven fibers was analyzed using the ImageJ (Image Processing and Analysis in Java) digital image analysis program. Average Co-Ni/PVA fiber diameters were found to be 190 nm. It was also

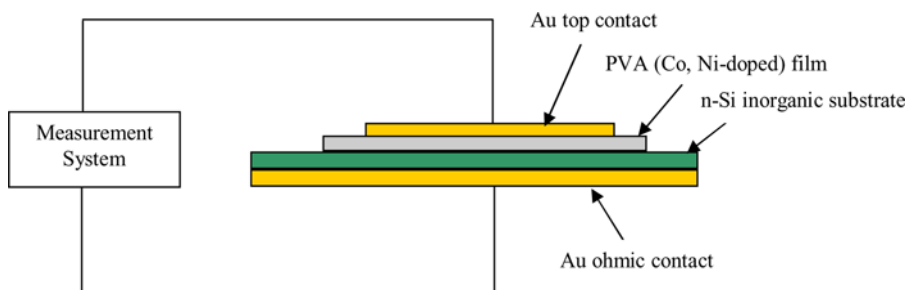


**Figure 3:** Schematic of Au/PVA (Co, Ni-doped)/n-Si Schottky diode and the measurement system.

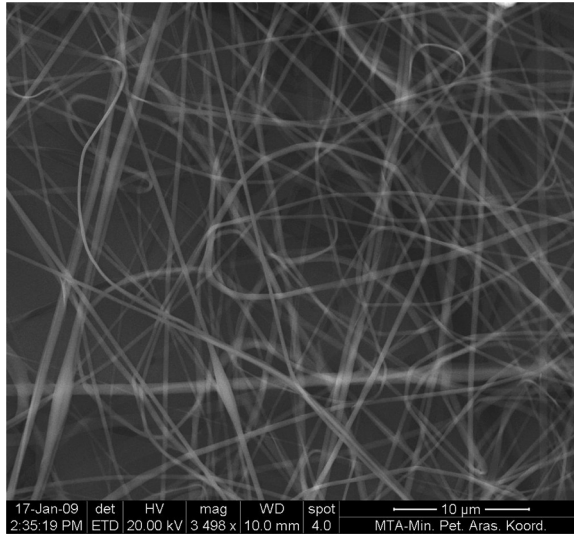


**Figure 4:** Selected SEM images of Au/PVA (Co, Ni-doped)n-Si Schottky diode.

observed that the Co-Ni/PVA nanofibers are highly linear, homogenous and showed no beading (Figure 4).

## RESULTS AND DISCUSSION

### Frequency Dependence of Dielectric Properties

Figure 5 shows the forward and reverse-bias  $C-V$  and  $G/\omega-V$  characteristics of Au/PVA (Co, Ni-doped) n-Si SDs, measured in the frequency range of 1 kHz–1 MHz at room temperature. The applied voltage range was between  $-1$  V and  $+6$  V. The three regimes of accumulation, depletion and inversion are clearly shown for each AC frequency. It can be seen from Figure 5(a) that, at low frequencies, the values of capacitance are shown to increase. The measured capacitance ( $C$ ) is dependent on bias voltage and frequency. One finding of interest, shown in Figure 5(a), is the two peaks observed in the  $C-V$  at low frequencies, especially around 1 V and 2 V, respectively. These peaks disappear when the frequency increases. The first peak, located at a low forward bias region due to the  $N_{ss}$  contribution, shifts from the high forward bias voltage to the low bias voltage as frequency increases. Also, the second peak shifts from the high forward bias voltage to the low bias voltage with increasing frequency. However, the SDs with high series resistance showed decreasing capacitance with increasing frequencies. The voltage and frequency dependence of  $C-V$  characteristics is due to the particular features of SD, impurity level, high series resistance, and doping density. This occurs because, at lower

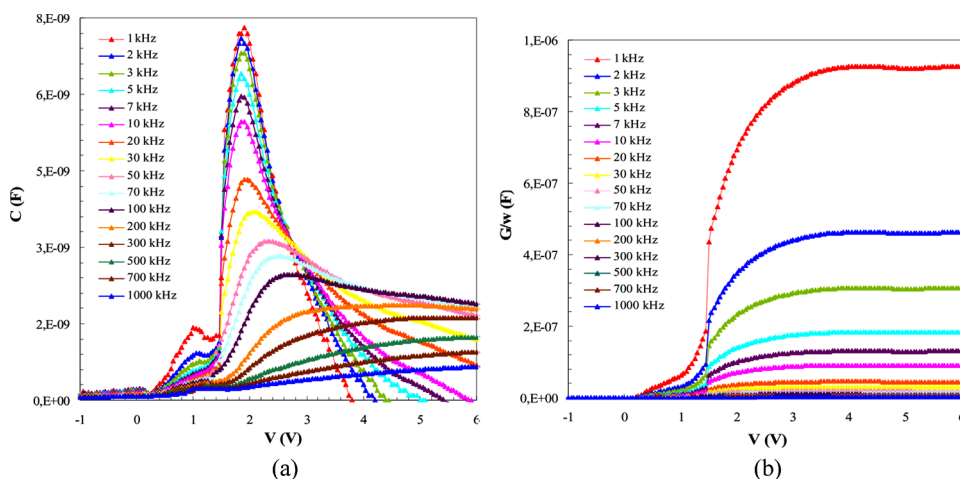


**Figure 5:** Variation of (a) measured capacitance ( $C$ ) and (b) conductance ( $G/\omega$ ) with gate bias at various frequencies for Au/PVA (Co, Ni-doped)/n-Si structure.

frequencies, the interface states can follow the AC signal and yield an excess capacitance, which depends on the frequency [22–24].

As shown in Figure 5(b),  $G/\omega-V$  is dependent on bias voltage and frequency.  $G/\omega-V$  is sensitive to frequency at relatively low frequency and increases with increasing frequency. Such behavior of the  $G/\omega-V$  is attributed to a particular distribution of surface states between Si-PVA (Co, Ni-doped) interfaces.

The frequency dependence of dielectric properties of bulk and films of PVA, PVA blends, and PVA doped with metal salts have studied by many researchers [2–11]. According to these studies, the dielectric constant of the PVA film increases with an increase in the frequency; this rate of increase is particularly high up to 100 Hz and then rapidly decreases at 1 kHz at a bias potential of 0 V. This may be due to polarization of the O-H chain molecule of PVA. The dipole orientation appears to be responsible for the changes occurring in the dielectric constant of typical high-polarity polymers such as PVA. Similarly, dielectric loss of PVA is maximum (1.81429) at a frequency of 20 Hz and at a bias potential of 40 V. The second maximum can be observed at a frequency of 100 Hz, after which the PVA dielectric loss trend decreases with a further increase in the frequency [10,25].

The most common method for measuring dielectric constant ( $\epsilon'$ ) and dielectric loss ( $\epsilon''$ ) consists of the capacitance  $C_0$  of an empty capacitor, the capacitance  $C_m$ , conductance  $G_m$ , and the resistance  $R_m = 1/G_m$  of the capacitor with the dielectric material in question. The measurement commonly involves the determination of the impedance of the circuit element formed by a cell containing the dielectric. The impedance can be defined in the following complex



form [26–29].

$$Z = \frac{1}{i\omega C_m + 1/R_m} = \frac{1}{i\omega R_m C_0 \varepsilon^*} \quad (1)$$

where,  $\omega$  is the angular frequency, and the complex permittivity ( $\varepsilon^*$ ) can be defined in the following form [30,31]:

$$\varepsilon^* = \varepsilon' - i\varepsilon'' \quad (2)$$

where,  $\varepsilon'$  and  $\varepsilon''$  are the real and the imaginary components of the complex dielectric constant. The real part of the dielectric constant ( $\varepsilon'$ ) at the various frequencies was calculated from Eq. (1) using the measured capacitance values ( $C_m$ ) at the strong accumulation region.

For substitution of Eq. (2) into Eq. (1), the real and the imaginary parts can be written as

$$\varepsilon' = \frac{C_m}{C_0} \quad (3)$$

$$\varepsilon'' = \frac{G_m}{\omega C_0} \quad (4)$$

where  $C_0$  is the capacitance of an empty capacitor,  $C_0 = \varepsilon_0(A/d)$ ,  $A$  is the rectifier contact area in  $\text{cm}^{-2}$ ,  $d$  is the interfacial insulator layer thickness, and  $\varepsilon_0$  is the permittivity of free space charge ( $\varepsilon_0 = 8,85 \times 10^{-14} \text{ F/cm}$ ). The imaginary part of the complex permittivity, the dielectric loss ( $\varepsilon''$ ), which is a measure of the loss of conductivity in the interfacial insulator layer at the various frequencies, is calculated using the measured conductance values from Eq. (4). In Eq. (4),  $\omega$  and  $C_m$  are the angular frequency and the measured conductance values, respectively. The loss tangent ( $\tan \delta$ ) is calculated from the relationship [32,33]:

$$\tan \delta = \frac{\varepsilon''}{\varepsilon'} \quad (5)$$

The AC electrical conductivity ( $\sigma_{ac}$ ) was computed using the relationship [34,35]:

$$\sigma_{ac} = \omega C \tan \delta (d/A) = \varepsilon'' \omega \varepsilon_0 \quad (6)$$

Many authors prefer to describe the dielectric properties of these devices by using the electric modulus formalization [31,36,37]. The complex permittivity ( $\varepsilon^* = 1/M^*$ ) data are transformed into the  $M^*$  formalism using the following relationship:

$$M^* = \frac{1}{\varepsilon^*} = M' + jM'' = \frac{\varepsilon'}{\varepsilon'^2 + \varepsilon''^2} + j \frac{\varepsilon''}{\varepsilon'^2 + \varepsilon''^2} \quad (7)$$

The frequency dependencies of the  $\epsilon'$ ,  $\epsilon''$  and  $\tan \delta$  of Au/PVA (Co, Ni-doped)n-Si SD at room temperature are shown in Figure 6(a–c), respectively. The values of the  $\epsilon'$ ,  $\epsilon''$  and  $\tan \delta$  were found to be strongly frequency-dependent. As can be seen from these figures, the values of  $\epsilon'$ ,  $\epsilon''$  and  $\tan \delta$  decrease as the frequency is increased. The decrease in  $\epsilon'$  and  $\epsilon''$  with increasing frequency is a general tendency and explained by the fact that, as the frequency is raised, the interfacial dipoles have less time to orientate themselves in the direction of the alternating field [38,39]. The peak value of the  $\epsilon'$  and  $\epsilon''$  stem from measurements of capacitance and conductance values, respectively, and such behaviors depend on a number of parameters, such as doping concentration, interface state density, series resistance of diode and the thickness of the interfacial insulator layer [33,40]. Typical values of  $\epsilon'$  and  $\epsilon''$  were 7.053, 702.252 at 1 kHz, and only 0.268, 1.155 at 1 MHz, respectively. These results show that the strong low-frequency dispersion that

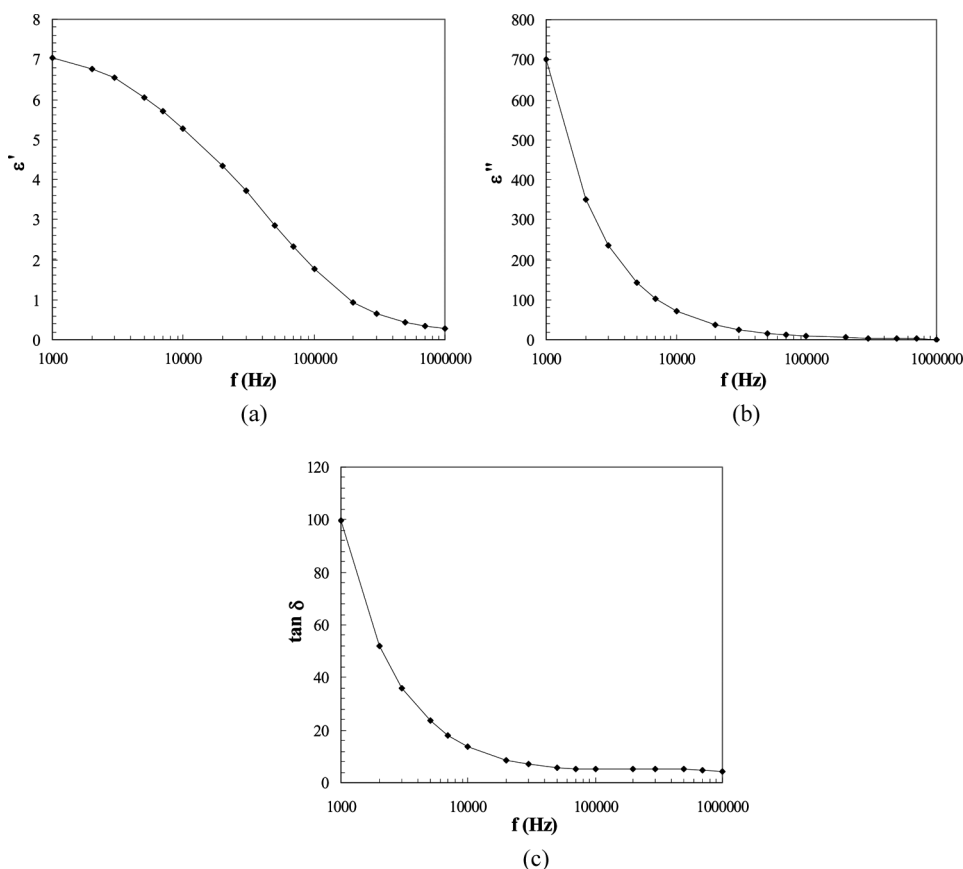


**Figure 6:** Frequency dependence of (a)  $\epsilon'$ , (b)  $\epsilon''$  and (c)  $\tan \delta$  at room temperature for Au/PVA (Co, Ni-doped)/n-Si structure.

characterizes the frequency-dependence of the  $\epsilon'$  and  $\epsilon''$  may, in general, be attributed to the four possible mechanisms at low frequency dielectric behavior of SDs: electrode interface, AC conductivity, dipole-orientation and charge carriers [41,42]. It is noted that, especially in the high frequency range (1 MHz), the values of  $\epsilon'$  become closer to the values of  $\epsilon''$ . This behavior of  $\epsilon'$  and  $\epsilon''$  may be due to the interface states, which can not follow the AC signal at high frequency. Figure 6(c) shows the variation of the loss tangent with respect to frequency for the structure. As shown in Figure 6(c), the  $\tan \delta$  decreases with increasing frequency but remains constant at high frequencies. This behavior is similar to behaviors of  $\epsilon'$  and  $\epsilon''$ . It is clear that  $\tan \delta$  is in closely related to the conductivity. The increase of the conductivity  $\sigma$  is accompanied by an increase of the eddy current, which in turn increases the energy loss  $\tan \delta$ . Figure 7 shows the variation of the AC conductivity  $\sigma_{ac}$  with frequency (in the frequency range 1 kHz to 1 MHz) at room temperature. It was noticed that the  $\sigma_{ac}$  decreases with decreasing frequency. It was noticed that the DC conductivity is generally increased with increasing frequency and there is a particularly sharp increase in the  $\sigma_{ac}$  after about 20 kHz. This behavior is typical for this structure and can be attributed to the space charge polarization [43–45] and a gradual decrease in series resistance with increasing frequency [23]. Figures 8(a) and (b) show the real part  $M'$  and the imaginary part  $M''$  of electric modulus  $M^*$  vs. frequency for Au/PVA (Co, Ni-doped)n-Si SD at 2 V bias voltages and room temperature. As can be seen from Figures 8(a) and (b),  $M'$  and  $M''$  increase as the frequency is increased and there is a particularly sharp increase in  $M'$  and  $M''$  in the frequency range

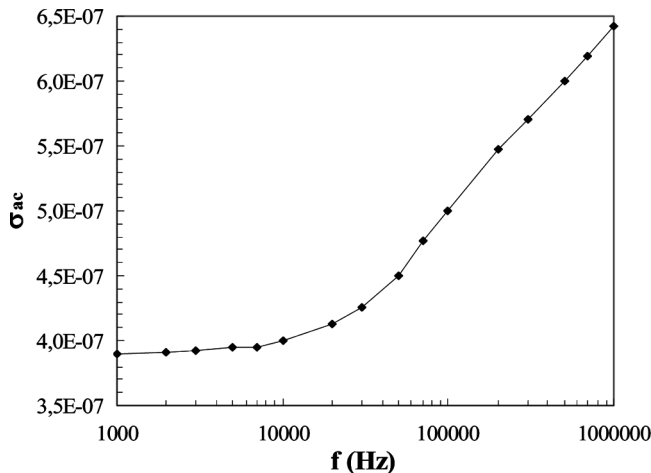


**Figure 7:** Frequency dependence of AC electrical conductivity ( $\sigma_{ac}$ ) for Au/PVA (Co, Ni-doped)/n-Si structure.

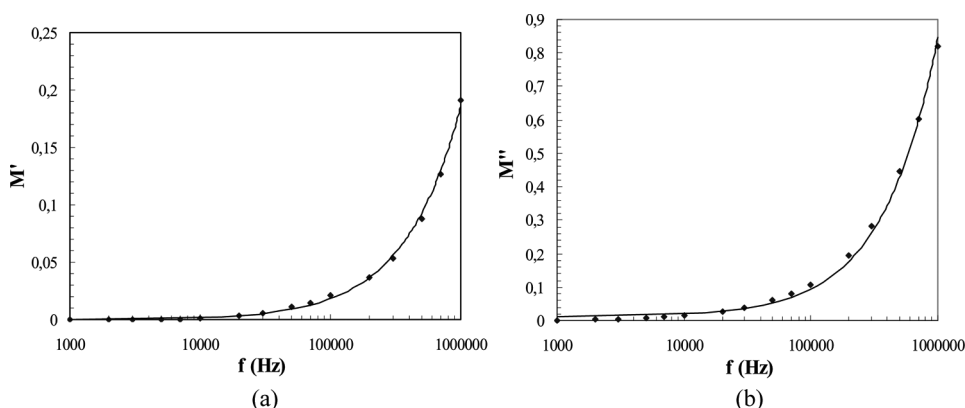


**Figure 8:** (a) Real part  $M'$  and (b) imaginary part  $M''$  of electric modulus  $M^*$  vs. frequency for Au/PVA (Co, Ni-doped)/n-Si structure.

between 50 kHz and 1 MHz. Similar findings have been reported in the literature [33,46].

## Temperature Dependence of Dielectric Properties

The temperature dependence of dielectric properties of PVA has been investigated extensively by many researchers. Salama et al. [2] reported that the variation of dielectric constant with temperature is different for polar and nonpolar polymers. Dielectric constant is independent of temperature for a nonpolar polymer, whereas for strong polar polymers, the dielectric constant increases with temperature. The increase of the dielectric constant with temperature is due to an increase of total polarization arising from dipoles and trapped charge carriers. However, since the specific volume of the polymer is temperature-dependent (i.e., it increases with temperature), the dielectric constant decreases with temperature in the case of weakly polar polymers. It is obvious that the dielectric constant increases with increasing temperature, which is attributed to the highly polar nature of PVA.

Figures 9 and 10 show the forward and reverse bias  $C-V$  and  $G/\omega-V$  characteristics of the structure, measured in the temperature range 80–400 K, for Au/PVA (Co, Ni-doped) n-Si SDs, at 1 MHz frequency. The capacitance and conductance are slightly sensitive to temperatures at low gate bias voltage. As seen in Figures 9(a) and 10(a), the capacitance and conductance are slightly dependent on temperature until 0 V. For this reason, it is understood that PVA (Co, Ni-doped) is a nonpolar polymer until 0 V. In the range of approximately 0–1.5 V, the capacitance and conductance increases slightly with temperature. At this range, PVA (Co, Ni-doped) shows slight polar characteristics. In the range of approximately 1.5–2 V, a phase transition is observed.

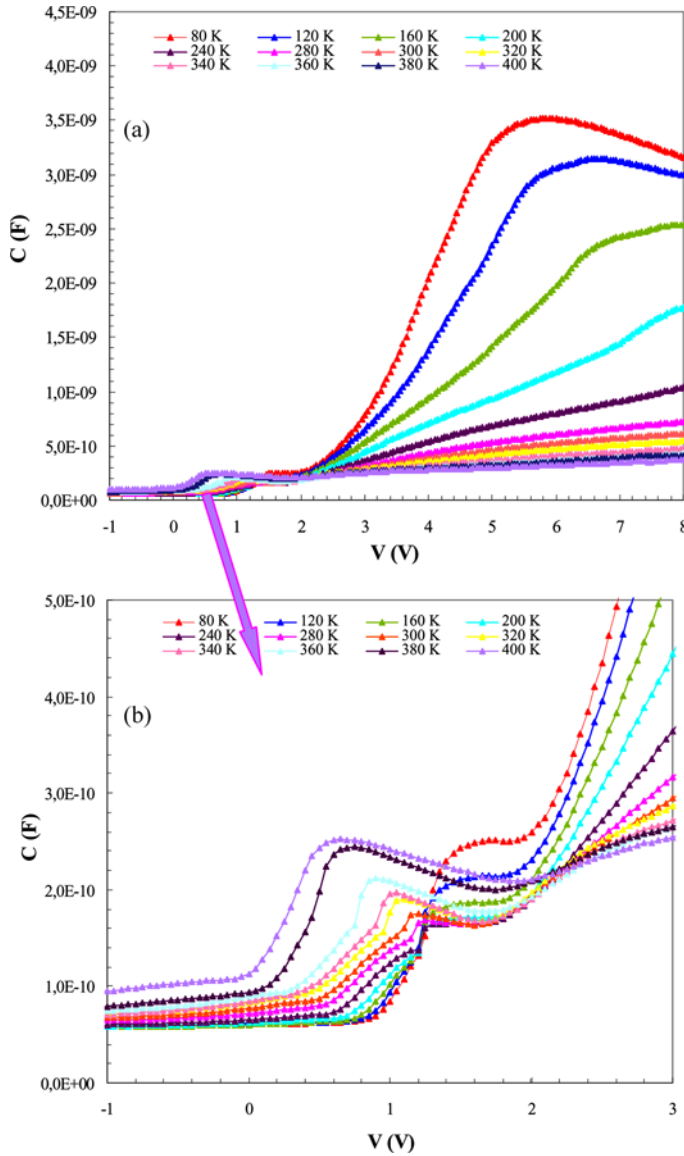


**Figure 9:** Variation of measured capacitance ( $C$ ) with gate bias at various temperatures for Au/PVA (Co, Ni-doped)/n-Si structure at (a) at  $-1$  to  $8$  V and (b)  $-1$  to  $3$  V.

Figure 9(b) and Figure 10(b) show  $C-V$  and  $G/\omega-V$  characteristics in the range of  $-1$  and  $2$  V. Above  $2$  V, the values of the capacitance and conductance show an interesting feature: the capacitance and conductance increase until a gate bias voltage (especially at low temperature), then decrease or stay constant. The rate of increase is very slight at high temperatures. This behavior may be due to

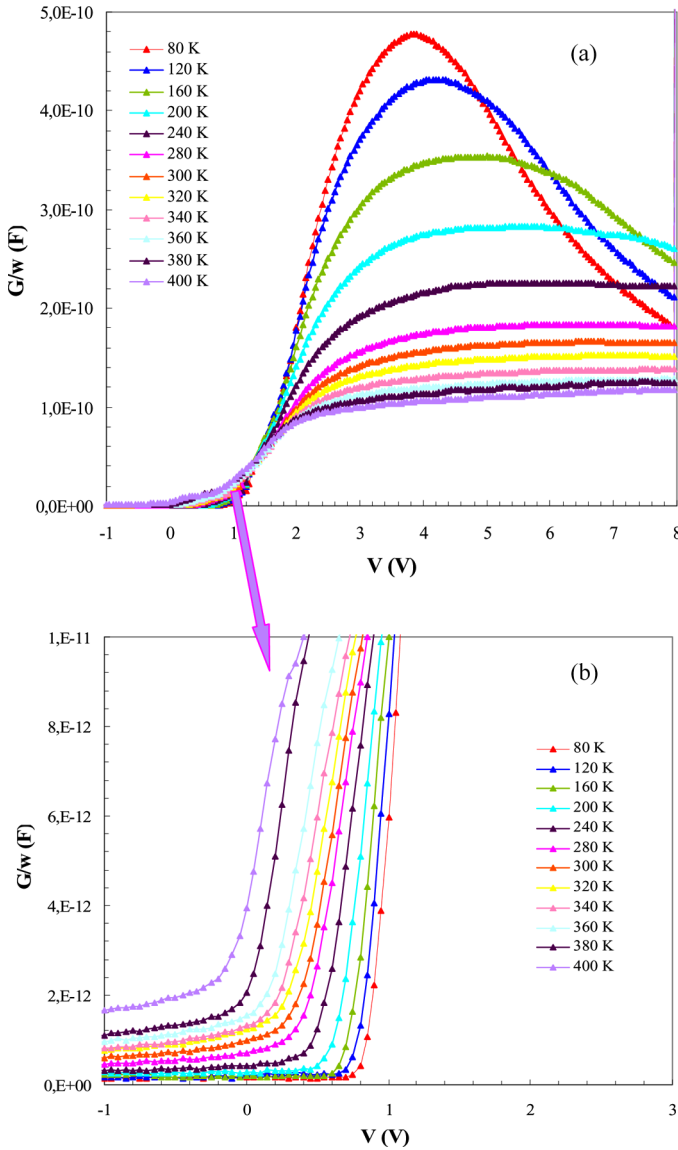


**Figure 10:** Variation of measured conductance ( $G/w$ ) with gate bias at various temperatures for Au/PVA (Co, Ni-doped)/n-Si structure at (a)  $-1$  to  $8$  V and (b)  $-1$  to  $3$  V.

polarization of the O-H chain molecule of PVA (Co, Ni-doped). While, PVA (Co, Ni-doped) shows weakly polar polymeric properties at high temperatures, it shows polar polymeric properties at low temperatures.

In this section of our study, the temperature dependence of dielectric constant ( $\epsilon'$ ), dielectric loss ( $\epsilon''$ ), loss tangent ( $\tan \delta$ ), AC electrical conductivity

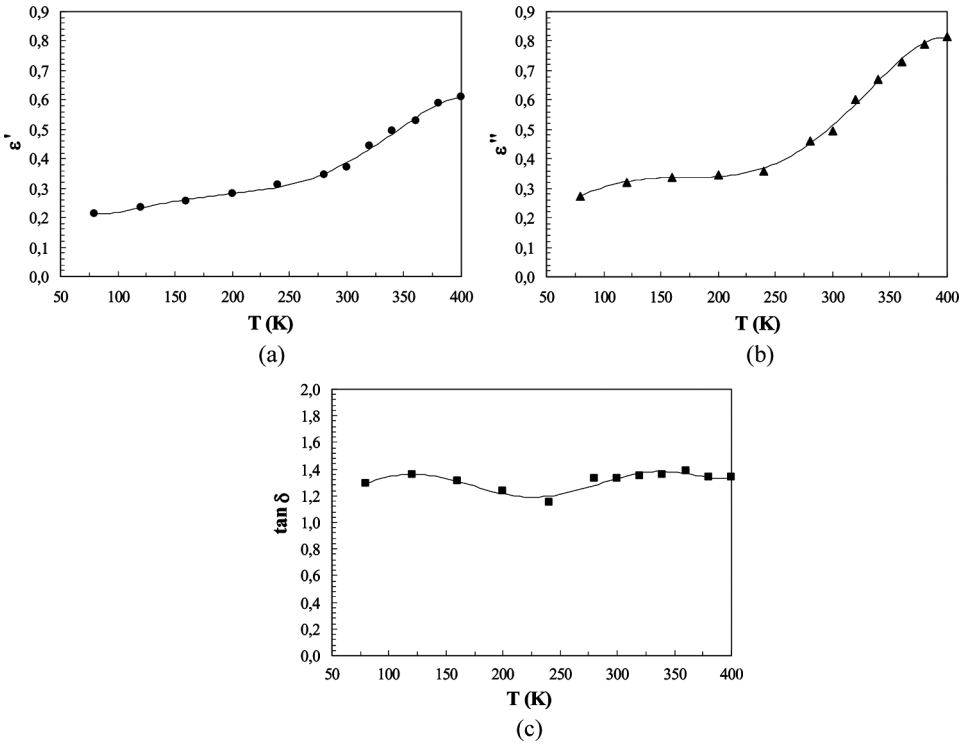


**Figure 11:** Temperature dependence of (a)  $\epsilon'$ , (b)  $\epsilon''$  and (c)  $\tan \delta$  at 1 MHz frequency for Au/PVA (Co, Ni-doped)/n-Si structure.

( $\sigma_{ac}$ ) and electric modulus were investigated for Au/PVA (Co, Ni-doped) n-Si Schottky diode. The dielectric properties are measured at high frequency (1 MHz) and temperature range (80–400 K). The variations of  $\epsilon'$  and  $\epsilon''$  with temperature at 1 MHz are shown in Figures 11(a) and (b), respectively. As can be seen from these figures, both  $\epsilon'$  and  $\epsilon''$  increase with increasing temperature, which is opposite to the effect of frequency. Similar findings have been reported in the literature for different materials [22,28,46]. Figure 11(c) shows the loss tangent ( $\tan \delta$ ) of Au/PVA (Co, Ni-doped)n-Si SD at a different voltage. As seen in Figure 11(c), the values of  $\tan \delta$  vs. temperature are almost constant except for a peak slightly at approximately 250 K. The variation of  $\epsilon'$ ,  $\epsilon''$  and  $\tan \delta$  with temperature is a general trend in ionic solids. It may be due to space charge polarization caused by impurities or interstitials in the materials. Moreover, in narrow band semiconductors, the charge carriers are not free to move but are trapped, causing a polarization. By increasing the temperature, the number of charge carriers increases exponentially and thus produces further space charge polarization and hence leads to a rapid increase in the dielectric constant  $\epsilon'$ . Both types of charge carriers (n and p) contribute to the polarization [23,29,47]. Furthermore, the increase in temperature induced

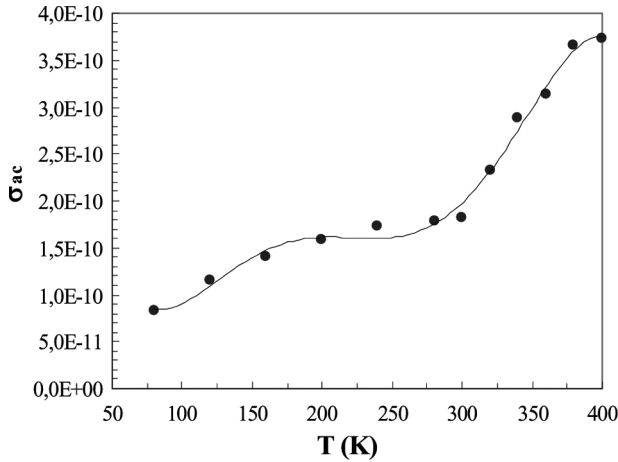


**Figure 12:** Temperature dependence of AC electrical conductivity ( $\sigma_{ac}$ ) for Au/PVA (Co, Ni-doped)/n-Si structure.

an expansion of molecules, which causes some increase in the electronic polarization and hence an increase in the  $\epsilon'$  and  $\epsilon''$  of the dielectric material [41,42].

The variation of the AC electrical conductivity ( $\sigma_{ac}$ ) with temperature Au/PVA (Co, Ni-doped) n-Si SD at a constant frequency of 1 MHz is shown in Figure 12. It is clear that the conductivity increases with increasing temperature, except within a temperature range of approximately 200–300 K. The curve of  $\sigma_{ac}$  is compatible with the curves of  $\epsilon'$  and  $\epsilon''$ . It can be noticed that the conductivity increases with increasing temperature until 200 K, followed by a phase approximately constant conductivity at a temperature range of 200–300 K. This phenomenon ensures the phase transition that may take place at this temperature range. After the transition, the mobility increases, owing to a considerable increase in the mobility of the free charges and the orientation and polarization of polar side groups in the chain units and, hence, the conductivity increases. The process of dielectric polarization in a metal-insulator-semiconductor (MIS) structure takes place through a mechanism similar to the conduction process. The increase in electrical conductivity at low temperature is attributed to the impurities, which reside at the grain boundaries [48,49]. These impurities lie below the bottom of the conduction band and thus have a small activation energy. This means that at low temperatures, the contribution to the conduction mechanism comes from the grain boundaries while, for higher temperatures, it mainly results from the grains.

Figures 13(a) and (b) show the real part  $M'$  and the imaginary part  $M''$  of electric modulus  $M^*$  vs. temperature for MIS SD at 1 MHz. As can be seen in Figure 13(a) and (b),  $M'$  and  $M''$  decrease with increasing temperature. On the other hand, Figure 13(a) shows that  $M'$  is relatively constant with increasing



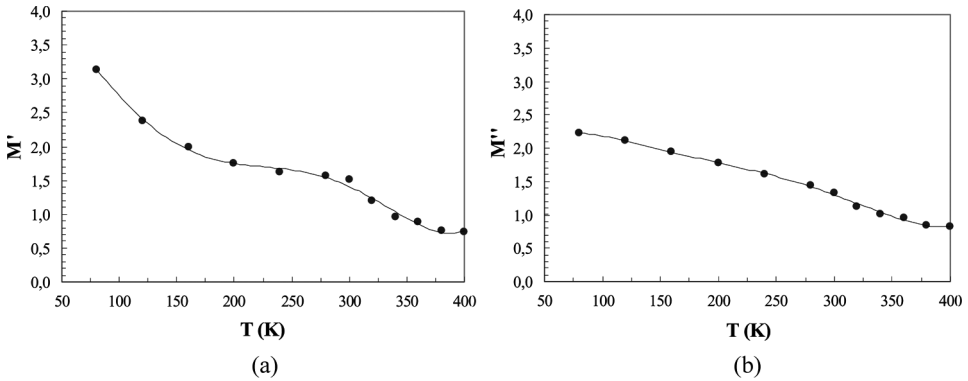


**Figure 13:** (a) Real part  $M'$  and (b) imaginary part  $M''$  of electric modulus  $M^*$  vs. temperature for Au/PVA (Co, Ni-doped)/n-Si structure.

temperature within temperature range 200 to 300 K. Similar findings have been reported in the literature [46,49,50].

## CONCLUSIONS

Frequency and temperature dependence of electrical and dielectric properties of Au/PVA (Co, Ni-doped) n-Si SD were studied in detail across wide temperature (80–400 K) and frequency (1 kHz–1 MHz) ranges. The values of capacitance ( $C$ ) and conductance ( $G/\omega$ ) show an interesting feature due to polarization of the PVA (Co, Ni-doped). The values of dielectric constant ( $\epsilon'$ ) and dielectric loss ( $\epsilon''$ ) increase with increasing temperature. Nonetheless, the values of dielectric constant ( $\epsilon'$ ) and dielectric loss ( $\epsilon''$ ) decrease with increasing frequency. Also, the AC electrical conductivity ( $\sigma_{ac}$ ) increases with increasing frequency and temperature, due to the accumulation of charge carriers at the boundaries. As a result, the behavior of dielectric properties depends particularly on frequency, interfacial insulator layer, the density of space charges, fixed surface charge and polarization of the PVA (Co, Ni-doped).

## REFERENCES

- [1] Sağlam, M., Biber, M., Türüt, A., Ağırtaş, M. S., and Çakar, M. *Int. J. Polym. Mater.* **54**, 805 (2005).
- [2] Salama, A. H., Dawy, M., and Nada, A. M. A. *Polym. Plast. Technol. Eng.* **43**, 1067 (2004).
- [3] Hanafy, T. A. *J. Appl. Polym. Sci.* **108**, 2540 (2008).
- [4] Ahmed, M. A., and Abo-Elhl, M. S. *J. Mater. Sci. Mater. Electron.* **9**, 391 (1998).

- [5] Anis, A., and Bantia, A. K. *Mater. Manufac. Process.* **22**, 737 (2007).
- [6] Hyon, S., Cha, W., and Ikada, Y. *Polym. Bull.* **22**, 119 (1989).
- [7] Wang, H. H., Shyr, T. W., and Hu, M. S. *J. Appl. Polym. Sci.* **74**, 3046 (1999).
- [8] Kanaya, T., Ohkura, M., Kaji, K., Furusaka, M., and Misawa, M. *Macromolecules* **27**, 609 (1994).
- [9] Uslu, İ., Daştan, H., Altaş, A., Yayli, A., Atakol, O., and Aksu, M. L. *e-Polymers* **13**, (2007).
- [10] Pawde, S. M., Deshmukh, K., and Parab, S. *J. Appl. Polym. Sci.* **109**, 1328 (2008).
- [11] Bhajantri, R. F., Ravindrachary, V., Harisha, A., Ranganathaiah, C., and Kumaraswamy, G. N. *Appl. Phys. A* **87**, 797 (2007).
- [12] Bur, A. J., and Roth, S. C. *J. Appl. Phys.* **57**, 113 (1985).
- [13] Sharma, A. K., and Ramu, C. *Mater. Sci. Eng.* **B15**, 222 (1992).
- [14] Mosad, M. M. *J. Mater. Sci. Lett.* **9**, 32 (1990).
- [15] Zhang, J., and Jiang, F. *Chem. Phys.* **289**, 243 (2003).
- [16] Moon, J., Park, J. A., Lee, S. J., Lim, S. C., and Zyung, T. *Current Appl. Phys.* **9**, S213 (2009).
- [17] Bazuev, G. V., Gyrdasova, O. I., Grigorov, I. G., and Koryakova, O. V. *Inorganic Materials* **41**, 288 (2005).
- [18] Watthanaarun, J., Pavarajarn, V., and Supaphol, P. *Sci. Tech. Adv. Mater.* **6**, 240 (2005).
- [19] Dökme, İ., Altındal, Ş., Tunç, T., and Uslu, İ. *Microelectron. Reliab.* **50**, 39 (2010).
- [20] Nicollian, E. H., and Goetzberger, A. *Appl. Phys. Lett.* **7**, 216 (1965).
- [21] Kar, S., and Varma, S. *J. Appl. Phys.* **58**, 4256 (1985).
- [22] Tataroğlu, A., and Altındal, S. *Microelectron. Eng.* **85**, 2256 (2008).
- [23] Tataroğlu, A., Altındal, S., and Bülbül, M. M. *Microelectron. Eng.* **81**, 140 (2005).
- [24] Tataroğlu, A., and Altındal, S. *Microelectron. Eng.* **83**, 582 (2006).
- [25] Joshi, G., and Pawde, S. M. *J. Appl. Polym. Sci.* **102**, 1014 (2006).
- [26] Chelkowski, A. (1980). *Dielectric Physics*, Elsevier, Amsterdam.
- [27] Symth, C. P. (1955). *Dielectric Behaviour and Structure*, McGraw-Hill, New York.
- [28] Von Hippel, A. R. (1954). *Dielectric Materials and Applications*, John Wiley & Sons Inc., New York.
- [29] Bülbül, M. M. *Microelectron. Eng.* **84**, 124 (2007).
- [30] Daniel, V. V. (1967). *Dielectric Relaxation*, Academic Press, London.
- [31] Afandiyeva, İ. M., Dökme, İ., Altındal, Ş., Bülbül, M. M., and Tataroğlu, A. *Microelectron. Eng.* **85**, 247 (2007).
- [32] Popescu, M., and Bunget, I. (1984). *Physics of Solid Dielectrics*, Elsevier, Amsterdam.
- [33] Dökme, İ., and Altındal, Ş. *Physica B: Condens. Mat.* **391**, 59 (2007).
- [34] Mattsson, M. S., Niklasson, G. A., Forsgren, K., and Harsta, A. *J. Appl. Phys.* **85**, 2185 (1999).

- [35] Dökme, İ., Altındal, Ş., and Gökçen, M. *Microelectron. Eng.* **85**, 1910 (2008).
- [36] Prabakar, K., Narayandass, S. K., and Mangalaraj, D. *Phys. Stat. Sol. (a)* **199**, 507 (2003).
- [37] Pissis, P., and Kyritsis, A. *Solid State Ion.* **97**, 105 (1997).
- [38] Prabakar, K., Narayandass, S. K., and Mangalaraj, D. *Phys. Stat. Sol. (a)* **199**, 507 (2003).
- [39] Sattar, A. A., and Rahman, S. A. *Phys. Stat. Sol. (a)* **200**, 415 (2003).
- [40] Chattopadhyay, P., and Raychaudhuri, B. *Solid State Electron.* **35**, 875 (1992).
- [41] Maurya, D., Kumar, J., and Shripal, R. P. T. *J. Phys. Chem. Solids* **66**, 1614 (2005).
- [42] Ranga Raju, M. R., Choudhary, R. N. P., and Ram, S. *Phys. State Sol. (b)* **239**, 480 (2003).
- [43] Szu, S. P., and Lin, C. Y. *Mater. Chem. Phys.* **82**, 295 (2003).
- [44] Migahed, M. D., Ishra, M., Fahmy, T., and Barakat, A. *J. Phys. Chem. Solids* **65**, 1121 (2004).
- [45] Sattar, A. A., and Rahman, S. A. *Phys. Status Solidi (a)* **200**, 415 (2003).
- [46] Tataroğlu, A., and Altındal, S. *Microelectron. Eng.* **85**, 1866 (2008).
- [47] Tataroğlu, A., Yücedağ, İ., and Altındal, S. *Microelectron. Eng.* **85**, 1518 (2008).
- [48] Gould, R. D., and Awan, S. A. *Thin Solid Films* **469**, 184 (2003).
- [49] Migahed, M. D., Ishra, M., Fahmy, T., and Barakat, A. *J. Phys. Chem. Solids* **65**, 1121 (2004).
- [50] Prabakar, K., Narayandass, S. K., and Mangalaraj, D. *Mater. Sci. Eng. B* **98**, 225 (2003).